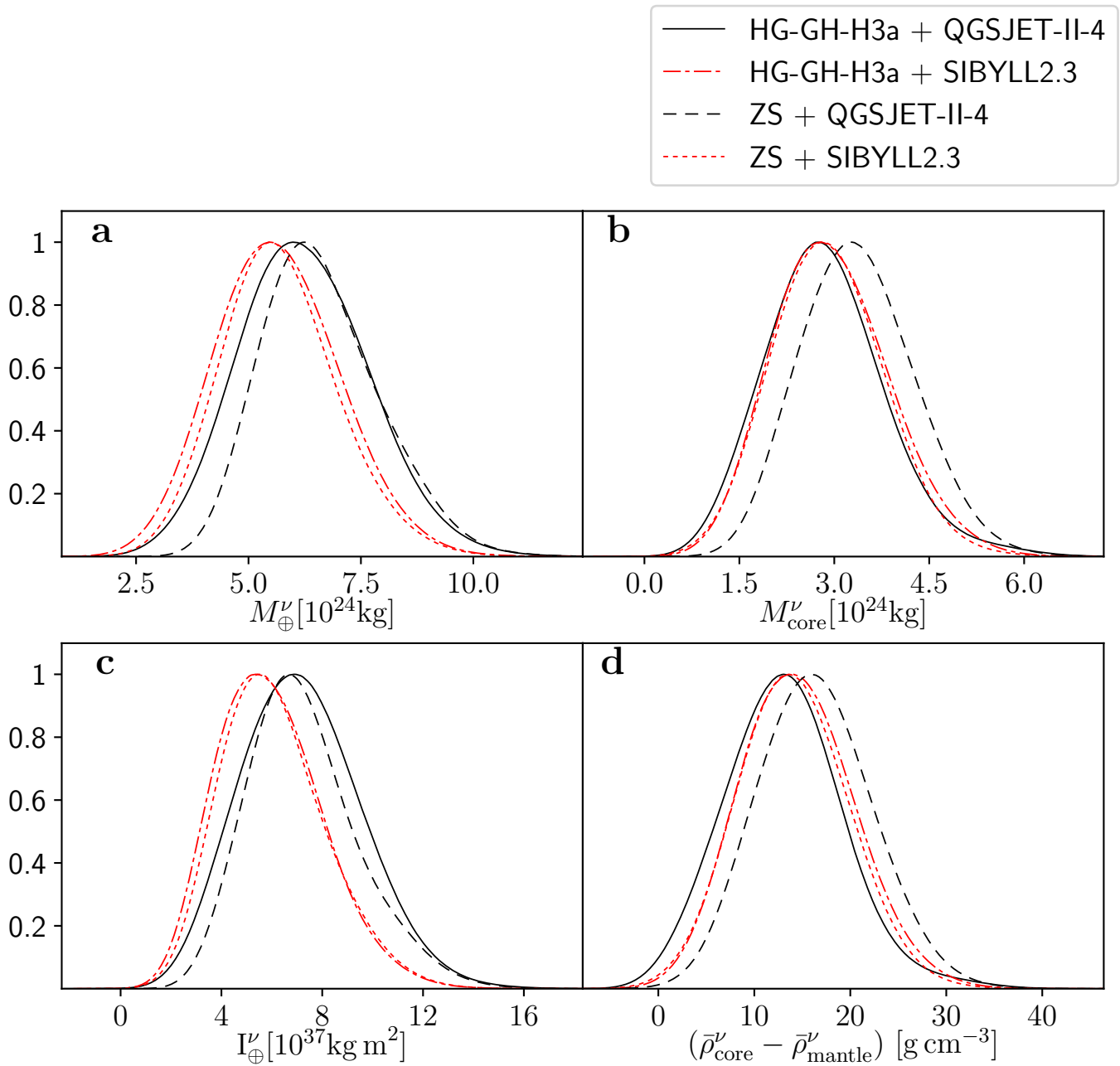


In the format provided by the authors and unedited.

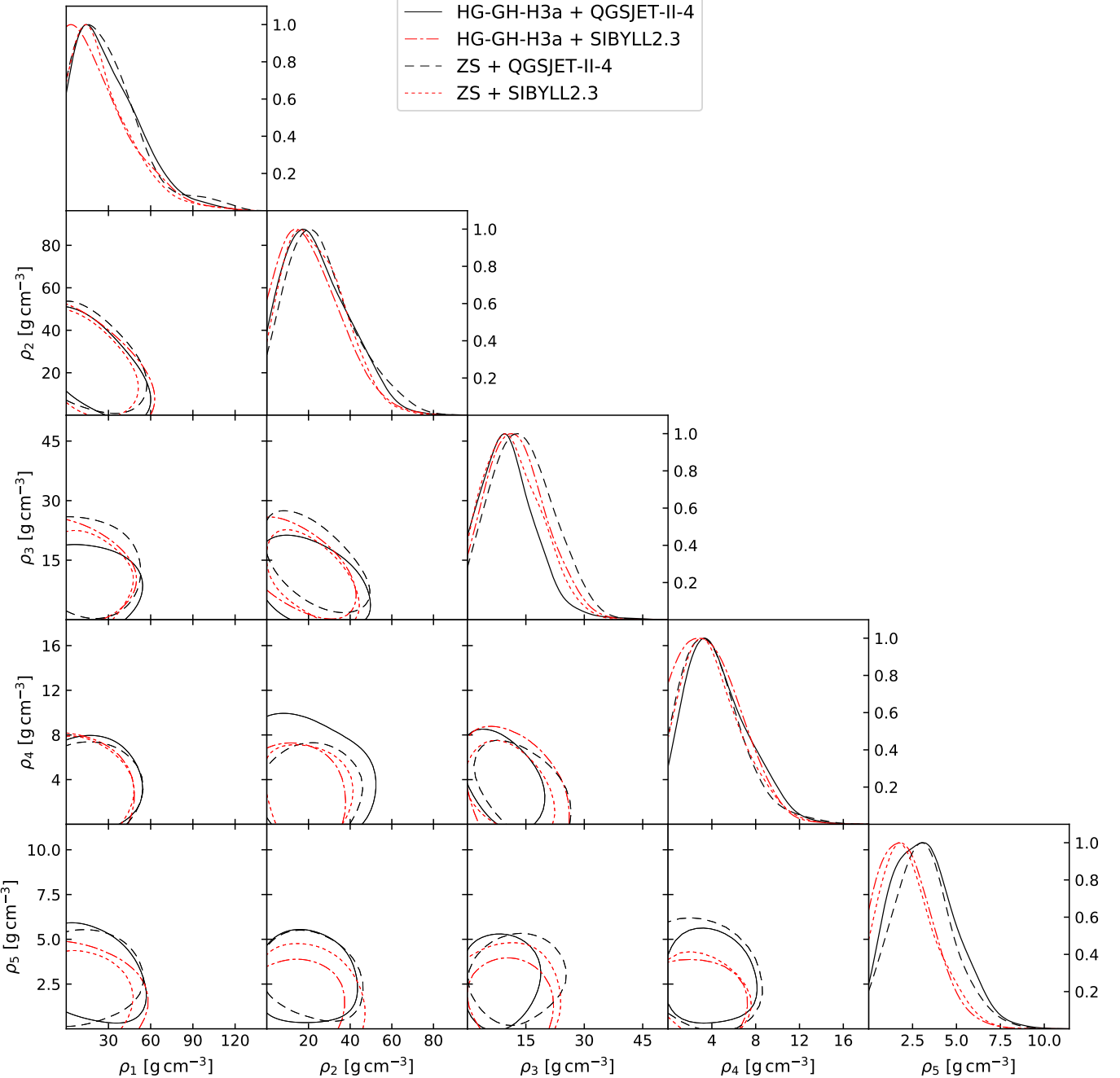
Neutrino tomography of Earth

Andrea Donini  ¹, Sergio Palomares-Ruiz  ^{1*} and Jordi Salvado  ^{1,2}

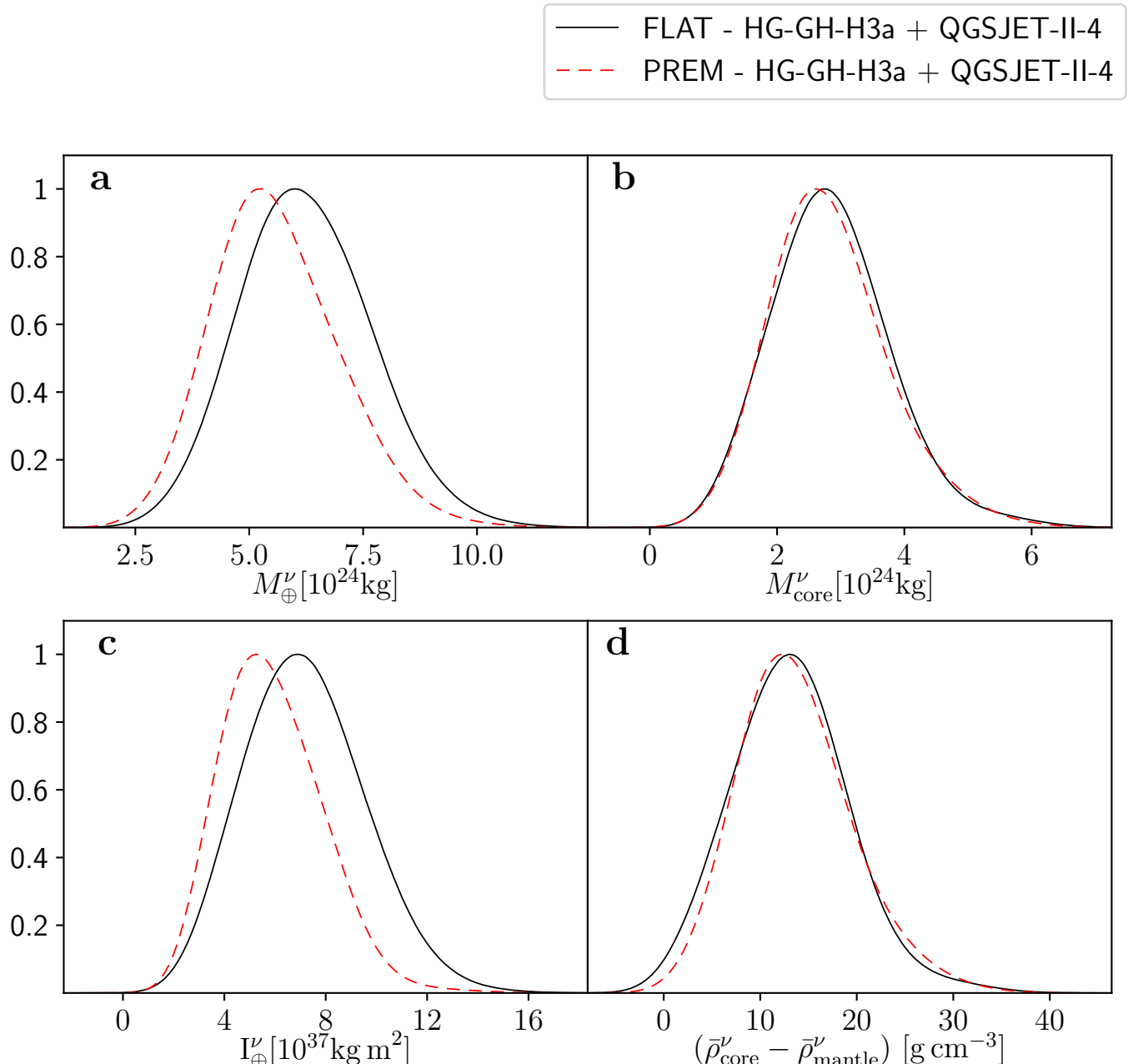
¹Instituto de Física Corpuscular (IFIC), CSIC-Universitat de València, Valencia, Spain. ²Departament de Física Quàntica i Astrofísica and Institut de Ciències del Cosmos, Universitat de Barcelona, Barcelona, Spain. *e-mail: sergiopr@ific.uv.es



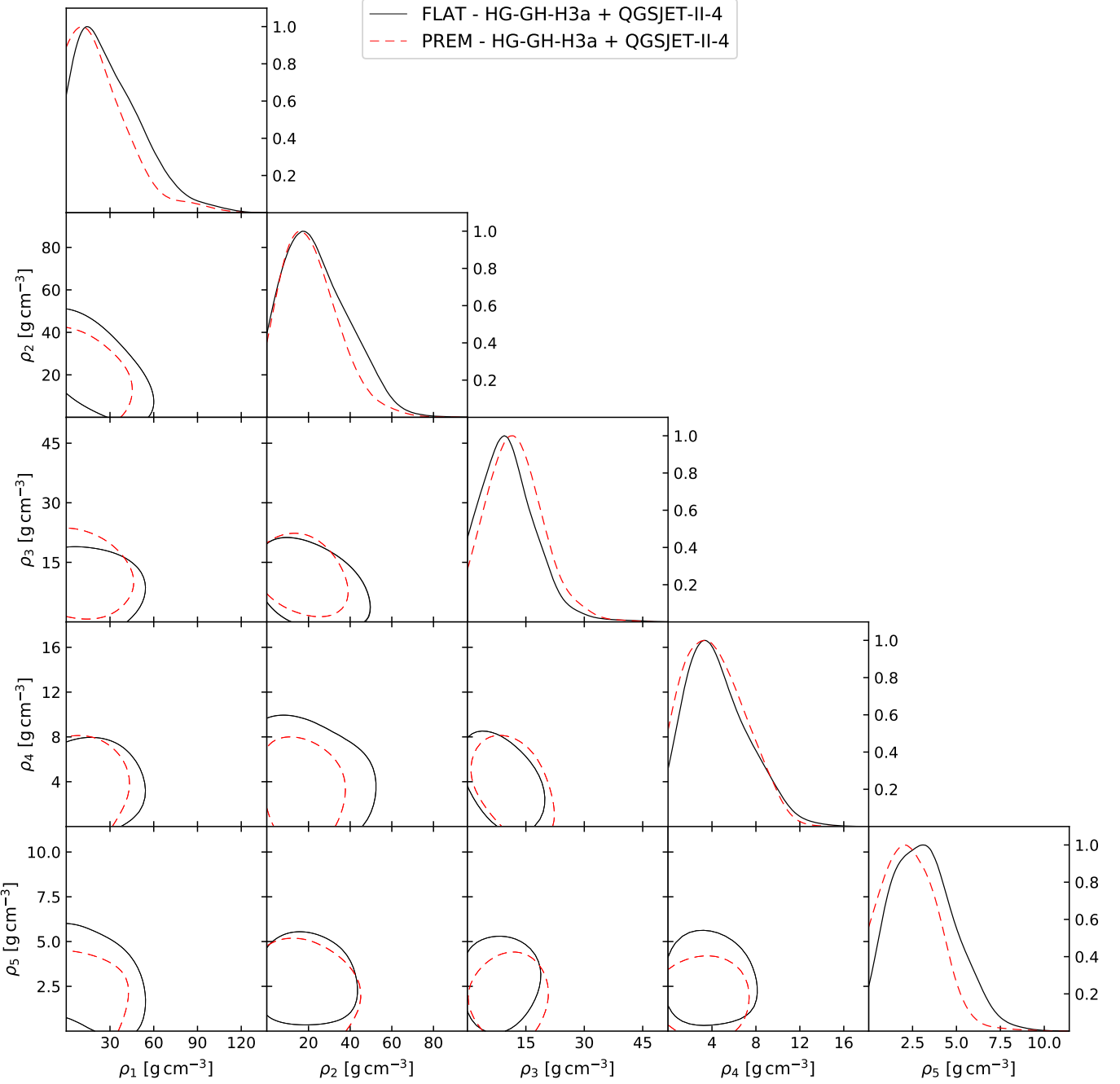
Supplementary Figure 1 | Systematic uncertainties among different atmospheric neutrino fluxes. Posterior probability distributions (normalized such that the maximum is 1) of the measured quantities for the Earth using neutrino tomography for four different atmospheric neutrino fluxes, resulting from the combinations of two primary cosmic-ray fluxes: the combined Honda-Gaisser primary cosmic-ray spectrum with the Gaisser-Hillas H3a correction (HG-GH-H3a) and the Zatsepin-Sokolskaya (ZS) spectrum, and two hadronic-interaction models, QGSJET-II-4 and SIBYLL2.3. All measurements are dominated by statistical uncertainties, being the systematics introduced by differences among atmospheric neutrino fluxes a subdominant effect. **a**, Earth's mass. **b**, Earth's core mass. **c**, Earth's moment of inertia. **d**, Difference of the average density between the Earth's core and mantle. The p -value for a mantle denser than the core corresponds to the area in the region where $\bar{\rho}_{\text{core}}^{\nu} \leq \bar{\rho}_{\text{mantle}}^{\nu}$. Our default model, HG-GH-H3a + QGSJET-II-4, has the larger p -value.



Supplementary Figure 2 | Posterior 68% probability contours for the densities of the Earth’s layers. We model the Earth with a piecewise flat profile, where each of the layers is described with constant density: ρ_1 corresponds to the inner core, ρ_2 and ρ_3 to the equal-thickness layers of the outer core, ρ_4 and ρ_5 to the equal-thickness layers of the mantle. We show the results for the four different combinations of primary cosmic-ray spectrum and hadronic-interaction model indicated in Methods and in Supplementary Fig. 1. With current data, the results are dominated by statistical uncertainties. On the rightmost panels, we depict the one-dimensional marginalized posterior probability distribution of the density of the layer corresponding to each column, normalized such that the maximum is 1.



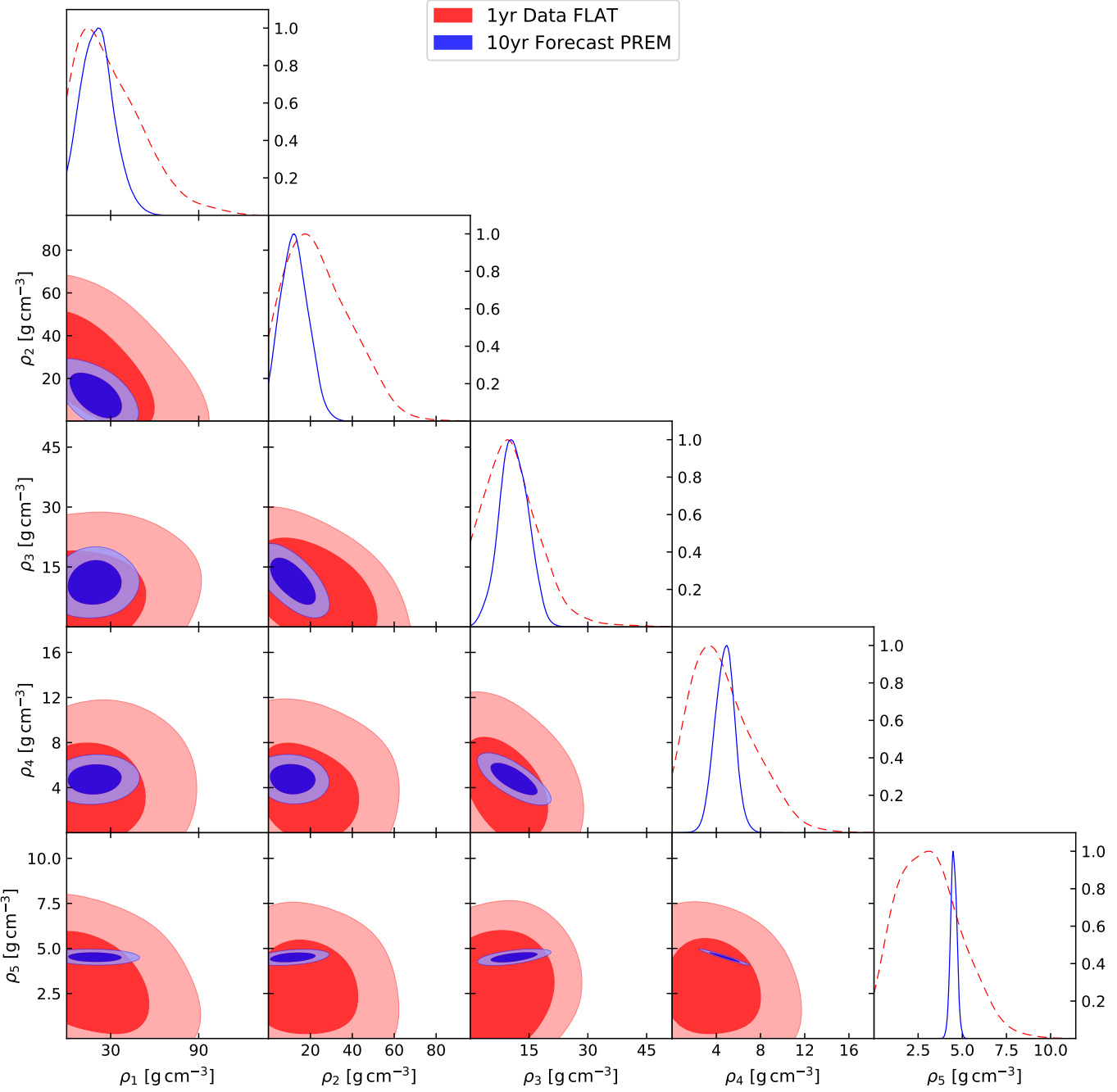
Supplementary Figure 3 | Systematic uncertainties between Earth density profiles. Posterior probability distributions (normalized such that the maximum is 1) of the measured quantities for the Earth using neutrino tomography for two different Earth's density profiles: a piecewise profile with five layers of constant density (as in Supplementary Fig. 1) and a five-layer model following the PREM profile. In all cases we use our default atmospheric neutrino fluxes: the combination of the Honda-Gaisser primary cosmic-ray spectrum with the Gaisser-Hillas H3a correction (HG-GH-H3a) and the QGSJET-II-04 hadronic-interaction model. **a**, Earth's mass. **b**, Earth's core mass. **c**, Earth's moment of inertia. **d**, Difference of the average density between the Earth's core and mantle.



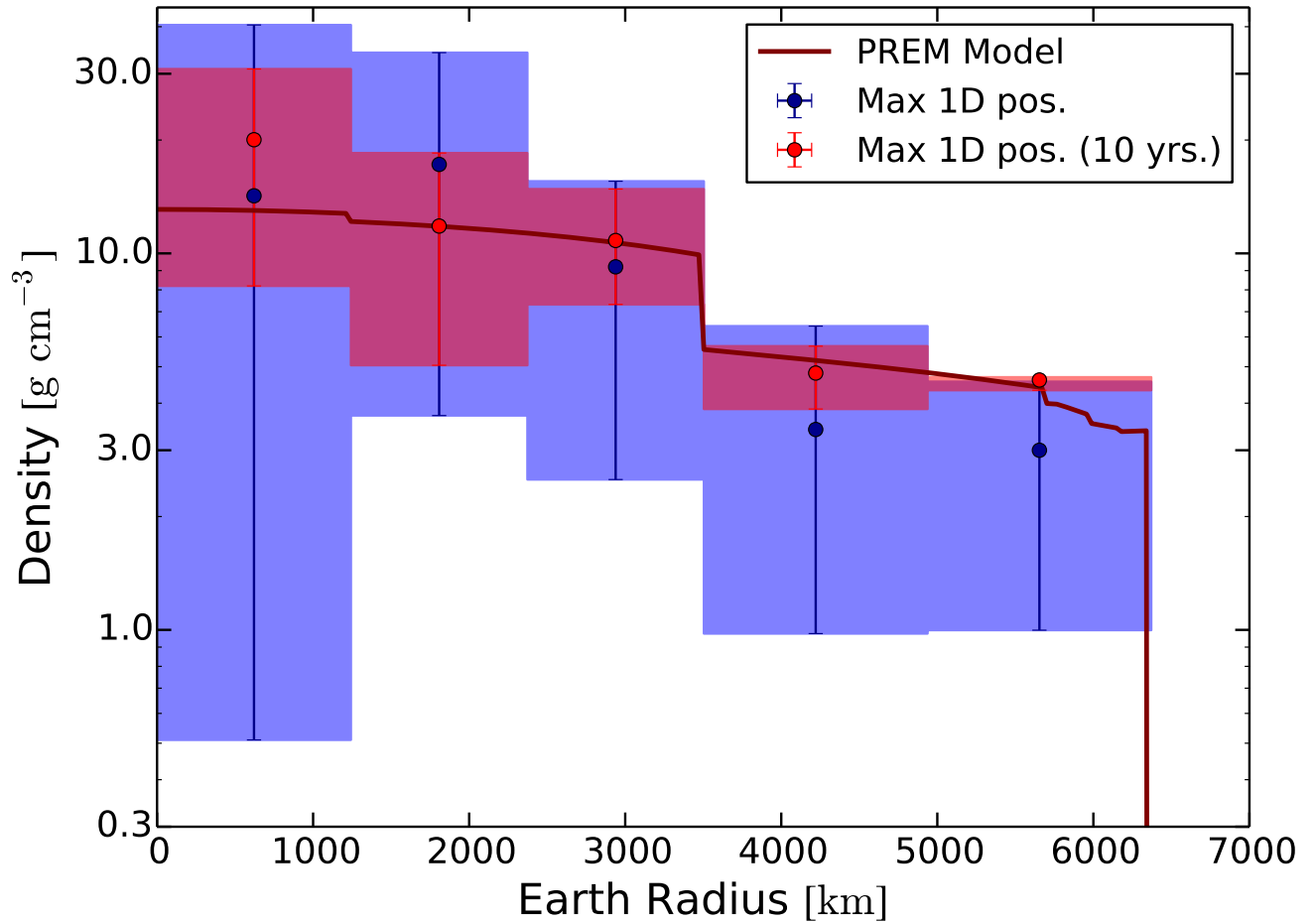
Supplementary Figure 4 | Posterior 68% probability contours for the densities of the five layers. We show the results for the densities of the layers corresponding to two different density profiles: a piecewise profile with five layers of constant density (as in Supplementary Fig. 2) and a five-layer model following the PREM profile. For the latter (non-constant density within the layers), the densities shown correspond to the value at the center of each layer. For the atmospheric neutrino fluxes, we consider the combination of the Honda-Gaisser primary cosmic-ray spectrum with the Gaisser-Hillas H3a correction (HG-GH-H3a) and the QGSJET-II-04 hadronic-interaction model. With current data, the results are dominated by statistical uncertainties. On the rightmost panels, we depict the one-dimensional marginalized posterior probability distribution of the parameter corresponding to each column, normalized such that the maximum is 1.

	Piecewise flat Earth's profile				PREM Earth's profile
	HG-GH-H3a + QGSJET-II-04	HG-GH-H3a + SIBYLL2.3	ZS + QGSJET-II-04	ZS + SIBYLL2.3	HG-GH-H3a + QGSJET-II-04
M_{\oplus}^{ν} [10 ²⁴ kg]	$6.0^{+1.6}_{-1.3}$	$5.5^{+1.5}_{-1.3}$	$6.2^{+1.4}_{-1.2}$	$5.5^{+1.3}_{-1.2}$	$5.3^{+1.5}_{-1.3}$
M_{core}^{ν} [10 ²⁴ kg]	$2.72^{+0.97}_{-0.89}$	$2.79^{+0.98}_{-0.85}$	$3.27^{+0.92}_{-0.89}$	$2.84^{+0.89}_{-0.88}$	$2.62^{+0.97}_{-0.84}$
I_{\oplus}^{ν} [10 ³⁷ kg cm ²]	6.9 ± 2.4	$5.4^{+2.3}_{-1.9}$	$6.7^{+2.3}_{-2.0}$	$5.5^{+2.2}_{-1.9}$	$5.3^{+2.3}_{-1.7}$
$\bar{\rho}_{\text{core}}^{\nu} - \bar{\rho}_{\text{mantle}}^{\nu}$ [g/cm ³]	$13.1^{+5.8}_{-6.3}$	$14.0^{+6.0}_{-5.9}$	$15.9^{+6.0}_{-5.9}$	$13.5^{+6.1}_{-5.5}$	$12.3^{+6.3}_{-5.4}$
p – value mantle denser than core	1.1×10^{-2}	2.4×10^{-3}	9.4×10^{-4}	4.6×10^{-3}	3.8×10^{-3}

Supplementary Table 1 | Results from neutrino tomography using one year of data (IC86 sample). Here we indicate the maximum of the posterior probability and the 68% credible interval (defined as the highest one-dimensional marginalized posterior density interval, see Methods) for each derived quantity: the Earth's mass, the Earth's core mass, the Earth's moment of inertia, and the difference in average density of the core and mantle. We also indicate the p –value for a mantle denser than the core ($\bar{\rho}_{\text{core}}^{\nu} \leq \bar{\rho}_{\text{mantle}}^{\nu}$). We show the results for four atmospheric neutrino fluxes assuming a piecewise profile with five constant-density layers and for a PREM-like profile with five layers, and the combination of the Honda-Gaisser primary cosmic-ray spectrum with the Gaisser-Hillas H3a correction (HG-GH-H3a) and the QGSJET-II-04 hadronic-interaction model.



Supplementary Figure 5 | Ten-year forecast versus current results. Posterior 68% and 95% probability contours for the densities of the five constant-density layers: ρ_1 corresponds to the inner core, ρ_2 and ρ_3 to the equal-thickness layers of the outer core, ρ_4 and ρ_5 to the equal-thickness layers of the mantle. We compare the results obtained with the current one-year IC86 data assuming a piecewise flat profile (red contours), with the forecast for 10 years (blue contours). For the forecast analysis, we simulate the future data assuming the PREM density profile and fit it with a model with five layers following the PREM profile in each layer (but with free normalization), so that the values indicated in the plots correspond to the central value in each of the layers. In all cases, for the atmospheric neutrino fluxes, we consider the combination of the Honda-Gaisser primary cosmic-ray spectrum with the Gaisser-Hillas H3a correction (HG-GH-H3a) and the QGSJET-II-04 hadronic-interaction model. For the forecast, we use the same systematic uncertainties that we have used throughout the paper. However, it is reasonable to think that they would be improved in the future. The outcome of the forecast is that, whereas with current data the results are dominated by statistical uncertainties, impressive improvements can be achieved already with a factor of ten larger statistics. The mantle density would be known with approximately five and ten times better precision for the lower and upper mantle, respectively, while the determination of the core density would improve by at least a factor of two, both for the inner and the outer core. Finally, note that currently more than seven years of data have already been collected, although data are not publicly available in the adequate form to perform this kind of analysis. On the rightmost panels, we depict the one-dimensional marginalized posterior probability distribution of the density of the layer corresponding to each column, normalized such that the maximum is 1.



Supplementary Figure 6 | Ten-year forecast versus current results: density profile. Fitted one-dimensional Earth's density profile with error bars representing 68% credible intervals (defined as the highest one-dimensional marginalized posterior density intervals, see Methods) and with the points with the highest one-dimensional marginalized posterior density indicated by dots. The blue bands and points represent the results obtained using current one-year (IC86) data and assuming the Earth is divided into five concentric layers of constant density (same as Fig. 3 in the main text). The red bands and points represent the expected results after ten years of observation. We have simulated the future data assuming the PREM density profile and fitted it with a model with five layers following the PREM profile in each layer (but with free normalization), so that the values indicated in the plots correspond to the central value in each of the layers. For the atmospheric neutrino fluxes, we consider the combination of the Honda-Gaisser primary cosmic-ray spectrum with the Gaisser-Hillas H3a correction (HG-GH-H3a) and the QGSJET-II-04 hadronic-interaction model. The purple curve represents the PREM density profile. Note that these results are obtained from one-dimensional marginalized posterior probability distributions and, therefore, correlations among all the parameters in the fit (five densities and four nuisance parameters) cannot be represented here. They give, therefore, a conservative representation of the allowed ranges for the density of individual layers.

Further references. Here we present a comprehensive list of references that have studied how to infer the internal structure of the Earth from effects on neutrino propagation in matter¹. There are three ways to do this. On one hand, the technique discussed in this work, neutrino absorption tomography, has been considered with neutrinos of different origins, such as man-made neutrinos^{2–17}, extraterrestrial neutrinos^{11,18–21} (first suggested by J. Learned and H. Bradner in the late 1970s) and atmospheric neutrinos^{22–26}. On the other hand, neutrino oscillation tomography, based on neutrino oscillations in matter, has been studied with man-made beams^{27–40}, with solar^{41–44}, atmospheric^{45–50} and supernova neutrinos^{42,51}, and general considerations have also been discussed^{52,53}. Finally, although technologically unfeasible, the diffraction pattern of Earth's matter caused by coherent neutrino scattering has also been studied^{54,55}.

Note that some of these references have also been quoted in the main text and in Methods, but they are indicated again here for the sake of completeness.

1. Winter, W. Neutrino tomography: Learning about the Earth's interior using the propagation of neutrinos. *Earth Moon Planets* **99**, 285–307 (2006). URL <https://doi.org/10.1007/s11038-006-9101-y>.
2. Placci, A. & Zavattini, E. On the possibility of using high-energy neutrinos to study the Earth's interior. *CERN Report* (1973). URL <https://cds.cern.ch/record/2258764>.
3. Volkova, L. V. & Zatsepin, G. T. On the problem of neutrino penetration through the Earth. *Izv. Akad. Nauk Ser. Fiz.* **38N5**, 1060–1063 (1974).
4. Nedelyakov, I. P. Experimental study of density distribution in celestial bodies by neutrino tomography method. *Compt. Rend. Acad. Bulgarian Sci.* **33**, 1615–1618 (1980).
5. Nedelyakov, I. P. Notes on neutrino tomography. *Compt. Rend. Acad. Bulgarian Sci.* **34**, 177–180 (1981).
6. Nedelyakov, I. P. A measurement system for determining Earth density distribution through its projection by neutrino beams. *Compt. Rend. Acad. Bulgarian Sci.* **34**, 493 (1981).
7. Nedelyakov, I. P. On the study of the Earth composition by means of neutrino experiments. *Balatonfured 1982, Proc. Neutrino '82* **1**, 300 (1981).
8. Nedelyakov, I. P. Measurement of projected mass density - A basic problem of neutrino geophysics. *Compt. Rend. Acad. Bulgarian Sci.* **36**, 1515–1518 (1983).
9. Krastev, A. & Nedelyakov, J. A numerical solution of the equation of the computerized tomography and its applications in astrophysics. *JINR E-11-83*, 692 (1983).
10. De Rújula, A., Glashow, S. L., Wilson, R. R. & Charpak, G. Neutrino exploration of the Earth. *Phys. Rept.* **99**, 341 (1983). URL [https://doi.org/10.1016/0370-1573\(83\)90108-4](https://doi.org/10.1016/0370-1573(83)90108-4).
11. Wilson, T. L. Neutrino tomography: Tevatron mapping versus neutrino sky. *Nature* **309**, 38–42 (1984). URL <https://doi.org/10.1038/309038a0>.
12. Askar'yan, G. A. Investigation of the Earth by means of neutrinos. Neutrino geology. *Sov. Phys. Usp.* **27**, 896–990 (1984). URL <https://doi.org/10.1070/PU1984v02n11ABEH004125>.
13. Volkova, L. V. Neutrino detection at large distances from accelerators. *Nuovo Cim.* **C8**, 552–578 (1985). URL <https://doi.org/10.1007/BF02582681>.
14. Tsarev, V. A. Geophysical applications of neutrino beams. *Sov. Phys. Usp.* **28**, 940 (1985). URL <https://doi.org/10.1070/PU1985v02n10ABEH003964>.
15. Borisov, A. B., Dolgoshein, B. A. & Kalinovsky, A. N. Direct method for determination of differential distribution of the Earth density by means of high-energy neutrino scattering. *Sov. J. Nucl. Phys.* **44**, 442 (1986). [Yad. Fiz. 44, 681–689 (1986)].
16. Tsarev, V. A. & Chechin, V. A. Long distance neutrino. Physical principles and geophysical applications. *Fiz. Elem. Chast. Atom. Yadra* **17**, 389–432 (1986).
17. Borisov, A. B. & Dolgoshein, B. A. Determination of rock density by means of high-energy neutrino beams by the delayed muon method. *Phys. Atom. Nucl.* **56**, 755–761 (1993).
18. Kuo, C., Crawford, H. J., Jeanloz, R., Romanowicz, B., Shapiro, G. & Stevenson, M. L. Extraterrestrial neutrinos and Earth structure. *Earth Planet. Sci. Lett.* **133**, 95–103 (1995). URL [https://doi.org/10.1016/0012-821X\(95\)00050-M](https://doi.org/10.1016/0012-821X(95)00050-M).
19. Crawford, H. J., Jeanloz, R. & Romanowicz, B. Mapping the Earth's interior with astrophysical neutrinos. *Proc. of the XXIV International Cosmic Ray Conference (University of Rome)* **1**, 804–807 (1995).
20. Jain, P., Ralston, J. P. & Frichter, G. M. Neutrino absorption tomography of the Earth's interior using isotropic ultrahigh-energy flux. *Astropart. Phys.* **12**, 193–198 (1999). URL [https://doi.org/10.1016/S0927-6505\(99\)00088-2](https://doi.org/10.1016/S0927-6505(99)00088-2).
21. Reynoso, M. & Sampayo, O. A. On neutrino absorption tomography of the Earth. *Astropart. Phys.* **21**, 315–324 (2004). URL <https://doi.org/10.1016/j.astropartphys.2004.01.003>.
22. González-García, M. C., Halzen, F., Maltoni, M. & Tanaka, H. K. M. Radiography of Earth's core and mantle with atmospheric neutrinos. *Phys. Rev. Lett.* **100**, 061802 (2008). URL <https://doi.org/10.1103/PhysRevLett.100.061802>.
23. Borriello, E. *et al.* Sensitivity on Earth core and mantle densities using atmospheric neutrinos. *JCAP* **0906**, 030 (2009). URL <https://doi.org/10.1088/1475-7516/2009/06/030>.
24. Borriello, E. *et al.* Studies on neutrino Earth radiography. *Earth Planets Space* **62**, 211–214 (2010). URL <https://doi.org/10.5047/eps.2009.06.004>.
25. Takeuchi, N. Simulation of heterogeneity sections obtained by neutrino radiography. *Earth Planets Space* **62**, 215–221 (2010). URL <https://doi.org/10.5047/eps.2009.05.004>.
26. Romero, I. & Sampayo, O. A. About the Earth density and the neutrino interaction. *Eur. Phys. J.* **C71**, 1696 (2011). URL <https://doi.org/10.1140/epjc/s10052-011-1696-0>.
27. Ermilova, V. K., Tsarev, V. A. & Chechin, V. A. Buildup of neutrino oscillations in the Earth. *JETP Lett.* **43**, 453–456 (1986). [Pisma Zh. Eksp. Teor. Fiz. 43, 353 (1986)].
28. Nicolaidis, A. Neutrinos for geophysics. *Phys. Lett.* **B200**, 553 (1988). URL [https://doi.org/10.1016/0370-2693\(88\)90170-0](https://doi.org/10.1016/0370-2693(88)90170-0).
29. Ermilova, V. K., Tsarev, V. A. & Chechin, V. A. Restoration of the density distribution of material based on neutrino oscillations. *Bull. Lebedev Phys. Inst.* **1988N3**, 51–54 (1988).
30. Nicolaidis, A., Jannane, M. & Tarantola, A. Neutrino tomography of the Earth. *J. Geophys. Res.* **96**, 21811–21817 (1991). URL <https://doi.org/10.1029/91JB01835>.
31. Ohlsson, T. & Winter, W. Reconstruction of the Earth's matter density profile using a single neutrino baseline. *Phys. Lett.* **B512**, 357–364 (2001). URL [https://doi.org/10.1016/S0370-2693\(01\)00731-6](https://doi.org/10.1016/S0370-2693(01)00731-6).
32. Ohlsson, T. & Winter, W. Could one find petroleum using neutrino oscillations in matter?. *Europhys. Lett.* **60**, 34–39 (2002). URL <https://doi.org/10.1209/epl/i2002-00314-9>.
33. Jacobsson, B., Ohlsson, T., Snellman, H. & Winter, W. Effects of random matter density fluctuations on the neutrino oscillation transition probabilities in the Earth. *Phys. Lett.* **B532**, 259–266 (2002). URL [https://doi.org/10.1016/S0370-2693\(02\)01580-0](https://doi.org/10.1016/S0370-2693(02)01580-0).
34. Winter, W. Probing the absolute density of the Earth's core using a vertical neutrino beam. *Phys. Rev.* **D72**, 037302 (2005). URL <https://doi.org/10.1103/PhysRevD.72.037302>.
35. Minakata, H. & Uchihama, S. On in situ determination of Earth matter density in neutrino factory. *Phys. Rev.* **D75**, 073013 (2007). URL <https://doi.org/10.1103/PhysRevD.75.073013>.

- 1 36. Gandhi, R. & Winter, W. Physics with a very long neutrino factory baseline. *Phys. Rev.* **D75**, 053002 (2007). URL <https://doi.org/10.1103/PhysRevD.75.053002>.
- 2 37. Wang, B., Chen, Y.-Z. & Li, X.-Q. Earthquake forecast via neutrino tomography. *Chin. Phys.* **C35**, 325-332 (2011). URL <https://doi.org/10.1088/1674-1137/35/4/002>.
- 3 38. Tang, J. & Winter, W. Requirements for a new detector at the South Pole receiving an accelerator neutrino beam. *JHEP* **1202**, 028 (2012). URL [https://doi.org/10.1007/JHEP02\(2012\)028](https://doi.org/10.1007/JHEP02(2012)028).
- 4 39. Argüelles, C. A., Bustamante, M. & Gago, A. M. Searching for cavities of various densities in the Earth's crust with a low-energy $\bar{\nu}_e$ β -beam. *Mod. Phys. Lett.* **A30**, 1550146 (2015). URL <https://doi.org/10.1142/S0217732315501461>.
- 5 40. Millhouse, M. A. & Latimer, D. C. Neutrino tomography. *Am. J. Phys.* **81**, 646-654 (2013). URL <https://doi.org/10.1119/1.4817314>.
- 6 41. Ioannissian, A. N. & Smirnov, A. Yu. Matter effects of thin layers: Detecting oil by oscillations of solar neutrinos. <https://arxiv.org/abs/hep-ph/0201012>.
- 7 42. Akhmedov, E. K., Tórtola, M. A. & Valle, J. W. F. Geotomography with solar and supernova neutrinos. *JHEP* **0506**, 053 (2005). URL <https://doi.org/10.1088/1126-6708/2005/06/053>.
- 8 43. Ioannissian, A., Smirnov, A. & Wyler, D. Oscillations of the ${}^7\text{Be}$ solar neutrinos inside the Earth. *Phys. Rev.* **D92**, 013014 (2015). URL <https://doi.org/10.1103/PhysRevD.92.013014>.
- 9 44. Ioannissian, A., Smirnov, A. & Wyler, D. Scanning the Earth with solar neutrinos and DUNE. *Phys. Rev.* **D96**, 036005 (2017). URL <https://doi.org/10.1103/PhysRevD.96.036005>.
- 10 45. Agarwalla, S. K., Li, T., Mena, O. & Palomares-Ruiz, S. Exploring the Earth matter effect with atmospheric neutrinos in ice. <https://arxiv.org/abs/1212.2238>.
- 11 46. Rott, C., Takeda, A. & Bose, D. Spectrometry of the Earth using neutrino oscillations. *Sci. Rep.* **5**, 15225 (2015). URL <https://doi.org/10.1038/srep15225>.
- 12 47. Winter, W. Atmospheric neutrino oscillations for Earth tomography. *Nucl. Phys.* **B908**, 250-267 (2016). URL <https://doi.org/10.1016/j.nuclphysb.2016.03.033>.
- 13 48. Bezrukov, L. & Sinev, V. Atmospheric neutrinos for investigation of Earth interior. *Phys. Part. Nucl.* **47**, 915-917 (2016). URL <https://doi.org/10.1134/S106377961606006X>.
- 14 49. Bourret, S., Coelho, J. A. B. & Van Elewyck, V. Neutrino oscillation tomography of the Earth with KM3NeT-ORCA. *J. Phys. Conf. Ser.* **888**, 012114 (2017). URL <https://doi.org/10.1088/1742-6596/888/1/012114>.
- 15 50. Naumov, P. Yu. & Sinev, V. V. Atmospheric neutrinos as a tool for exploring the Earth's inner parts. *Phys. Atom. Nucl.* **80**, 1171-1176 (2017). URL <https://doi.org/10.1134/S106377881706014X>.
- 16 51. Lindner, M., Ohlsson, T., Tomàs, R. & Winter, W. Tomography of the Earth's core using supernova neutrinos. *Astropart. Phys.* **19**, 755-770 (2003). URL [https://doi.org/10.1016/S0927-6505\(03\)00120-8](https://doi.org/10.1016/S0927-6505(03)00120-8).
- 17 52. Koike, M., Ota, T., Saito, M. & Sato, J. Parametric resonance in neutrino oscillation: A guide to control the effects of inhomogeneous matter density. *Phys. Lett.* **B759**, 266-271 (2016). URL <https://doi.org/10.1016/j.physletb.2016.05.083>.
- 18 53. Ioannissian, A. N. & Smirnov, A. Yu. Attenuation effect and neutrino oscillation tomography. *Phys. Rev.* **D96**, 083009 (2017). URL <https://doi.org/10.1103/PhysRevD.96.083009>.
- 19 54. Fortes, A. D., Wood, I. G. & Oberauer, L. Using neutrino diffraction to study the Earth's core. *Astron. Geophys.* **47**, 5.31-5.33 (2006). URL <https://doi.org/10.1111/j.1468-4004.2006.47531.x>.
- 20 55. Lauter, R. Diffraction of solar neutrinos at the Earth's solid core. *Astron. Nachr.* **338**, 111-116 (2017). URL <https://doi.org/10.1002/asna.201613049>.